On Computational Issues of Market-Based Optimal Power Flow

Hongye Wang, *Student Member, IEEE*, Carlos E. Murillo-Sánchez, *Member, IEEE*, Ray D. Zimmerman, *Member, IEEE*, and Robert J. Thomas, *Fellow, IEEE*

***Abstract*—The deregulated electricity market calls for robust optimal power flow (OPF) tools that can provide a) deterministic convergence; b) accurate computation of nodal prices; c) support of both smooth and nonsmooth costing of a variety of resources and services, such as real energy, reactive energy, voltages support, etc.; d) full active and reactive power flow modeling of large-scale systems; and e) satisfactory worst-case performance that meets the real-time dispatching requirement. Most prior research on OPF has focused on performance issues in the context of regulated systems, without giving much emphasis to requirements a)–c). This paper discusses the computational challenges brought up by the deregulation and attempts to address them through the introduction of new OPF formulations and algorithms. Trust-region-based augmented Lagrangian method (TRALM), step-controlled primal-dual interior point method (SCIPM), and constrained cost variable (CCV) OPF formulation are proposed. The new formulations and algorithms, along with several existing ones, are tested and compared using large-scale power system models.**

***Index Terms*—Augmented Lagrangian method, constrained cost variable, economic dispatch, electricity market, market-based optimal power flow, multiplier method, nonsmooth optimization, optimal power flow, primal-dual interior point method, step-controlled interior point method, trust region method.**

I. Introduction

THE optimal power flow (OPF) problem has been one of the most widely studied subjects in the power system community since Carpentier first published the concept in 1962 [1]. Over the years, researchers have examined various algorithmic techniques that seek to speed up the OPF computation. References [2]–[6] captured most of the work done in the 1970s and the 1980s, a time when several constrained optimization techniques such as Lagrange multiplier methods, penalty function methods, and sequential quadratic programming, coupled with gradient methods and Newton methods for unconstrained optimization, emerged as the leading nonlinear programming (NLP) algorithms for solving AC OPFs. In recent years, algorithms based on the primal-dual interior point method (PDIPM) have gained popularity [7]–[13].

Despite the advancements being made, the full AC OPF has not been widely adopted in real-time operations of large-scale power systems. Instead, system operators often use simplified OPF tools that are based on linear programming (LP) and decoupled (DC) system models [14]. Historically, this is mainly due to the lack of powerful computer hardware and efficient AC OPF algorithms. With the advent of fast low-cost computers, however, speed has now become a secondary concern, after algorithm robustness. The remaining prevalent argument for using LP-based DC OPF instead of NLP-based AC OPF is that LP algorithms are deterministic and always yield solutions, albeit not necessarily the desired ones, while NLP algorithms are less robust and often experience convergence problems.

The emergence of deregulated electricity markets poses new challenges to the solution of the OPF problem. Unlike in the regulated system, where the goal of computing the OPF is merely minimizing the smooth quadratic cost of real energy production, OPF computation is now part of the core pricing mechanism for electricity trading in deregulated markets, where real energy, reactive energy, voltage support, and other system resources and services can all be traded in discrete bids and offers [14]–[16]. In order to meet their legal obligations of providing timely market settlements and to ensure market fairness and efficiency, independent system operators (ISOs) must adopt OPF tools that provide a) deterministic convergence; b) accurate computation of nodal prices; c) support of both smooth and nonsmooth costing of a variety of resources and services, such as real energy, reactive energy, voltage support, etc.; d) full active and reactive power flow modeling of large-scale systems; and e) satisfactory worst-case performance that meets the real-time dispatching requirement. Most prior research on OPF has focused on performance issues in the context of regulated systems, without giving much emphasis to requirements a)–c).

In this paper, we look into the computational challenges brought up by the deregulation and seek to address them through new algorithms and new OPF formulations. Three separate techniques, namely, trust-region based augmented Lagrangian method (TRALM), step-controlled primal-dual interior point method (SCIPM), and constrained cost variable (CCV) OPF formulation, are proposed here for reliable and efficient computation of large-scale market-based OPFs. TRALM integrates the well-proven penalty and augmented Lagrangian method [21] with the trust-region unconstrained optimization technique [17]–[21] to achieve algorithm robustness. SCIPM amends the popular primal-dual interior point method with a step control procedure to enhance the convergence of market-based OPF computation. TRALM is more theoretically

Manuscript received November 7, 2006; revised March 4, 2007. This work was supported in part by the National Science Foundation under Award 0532744. Paper no. TPWRS-00796-2006.

H. Wang, R. D. Zimmerman, and R. J. Thomas are with the School of Electrical and Computer Engineering, Cornell University, Ithaca, NY 14850 USA (e-mail: hw41@cornell.edu; rz10@cornell.edu; rjt1@cornell.edu).

C. E. Murillo-Sánchez is with Universidad Autónoma de Manizales, Manizales, Colombia (e-mail: cmurillo@autonoma.edu.co).

Color versions of one or more of the figures in this paper are available online at http://ieeexplore.ieee.org.

Digital Object Identifier 10.1109/TPWRS.2007.901301

rigid, but in terms of computational performance, SCIPM is better for real-time applications. CCV is an alternative OPF formulation that we propose to improve the scalability of market-based OPF computation. It embeds market-induced piecewise cost functions into inequality constraints as opposed to the objective function. Section II of this paper presents the classical AC OPF formulation and defines metrics that will be used for accuracy comparisons of various methods. TRALM and SCIPM are then introduced in Section III. Section IV discusses two alternative OPF formulations, including the newly proposed CCV. In Section V, we show numerical results and compare OPF algorithms and formulations using several different power system models. This paper is then concluded in Section VI.

II. Problem Formulation

The classical AC OPF formulation can be written as

$$\min_{P,Q,V,\theta} \quad C(P,Q,V,\theta) \tag{1a}$$

$$\text{s.t.} \quad FA_i(P,V,\theta)=0; FR_i(Q,V,\theta)=0 \tag{1b}$$

$$P_j^{\min} \le P_j \le P_j^{\max}; Q_j^{\min} \le Q_j \le Q_j^{\max} \tag{1c}$$

$$V_i^{\min} \le V_i \le V_i^{\max} \tag{1d}$$

$$|SF_k(V,\theta)|^2 \le (S_k^{\max})^2 \tag{1e}$$

$$|ST_k(V,\theta)|^2 \le (S_k^{\max})^2 \tag{1f}$$

$$i \in [1, N_{bus}]; j \in [1, N_{gen}]; k \in [1, N_{line}] \tag{1g}$$

where (1a) is the objective function representing the system cost, (1b) includes the nodal real and reactive power balancing equations, (1c) and (1d) are the constraints on generations and bus voltages, and (1e) and (1f) are squared branch flow constraints. Bounds in inequality constraints (1c)–(1f) are typically supplied by unit commitment and security analysis tools in real-time system operations. In this study, we choose to use the default bounds that come with our sample power system data. Changes in price-sensitive loads, transformer taps, and switching shunt capacitors are not modeled in this work but can be accommodated through additional control variables.

The Lagrangian of (1) is written as

$$\begin{aligned} L = {} & C(P,Q,V,\theta) + \lambda_{FA}^T FA(P,V,\theta) + \lambda_{FR}^T FR(Q,V,\theta) \\ & + \mu_{P+}^T (P - P^{\max} + Z_{P+}) + \mu_{P-}^T (P^{\min} - P + Z_{P-}) \\ & + \mu_{Q+}^T (Q - Q^{\max} + Z_{Q+}) + \mu_{Q-}^T (Q^{\min} - Q + Z_{Q-}) \\ & + \mu_{V+}^T (V - V^{\max} + Z_{V+}) + \mu_{V-}^T (V^{\min} - V + Z_{V-}) \\ & + \mu_{SF}^T \left(|SF(V,\theta)|^2 - (S^{\max})^2 + Z_{SF} \right) \\ & + \mu_{ST}^T \left(|ST(V,\theta)|^2 - (S^{\max})^2 + Z_{ST} \right) \end{aligned} \tag{2}$$

where Z's are slack variables and λ's and μ's are the Lagrange multipliers that are used in the market to price various kinds of electricity transactions. For example, λ_{FA} is the vector of real-energy nodal prices. Given the exact or a benchmark solution of the first-order and second-order Karush–Kuhn–Tucker (KKT) conditions of (2)

$$\left(C^*, P^*, Q^*, V^*, \theta^*, \lambda_{FA,FR}^*, \mu_{P\pm,Q\pm,V\pm,SF,ST}^* \right)$$

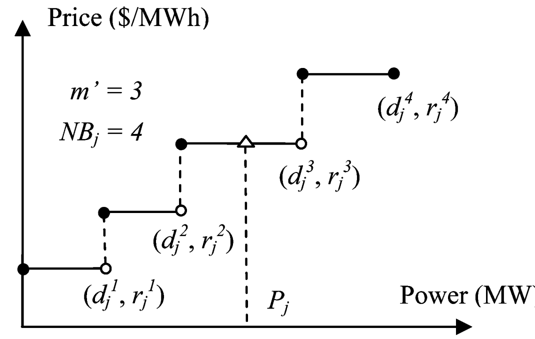

Fig. 1. Example discrete price-power curve for market-based OPF.

and a solution generated by a new OPF tool under study

$$\left(C, P, Q, V, \theta, \lambda_{FA,FR}, \mu_{P\pm,Q\pm,V\pm,SF,ST} \right)$$

we can use the following metrics to verify the legitimacy of the new tool:

$$\delta_C \equiv \max\left(|C - C^*| / (1 + |C^*|) \right) \tag{3a}$$

$$\delta_X \equiv \max\left(\left\| [(P^* + e)]^{-1} (P - P^*) \right\|_\infty \; \left\| [(V^* + e)]^{-1} (V - V^*) \right\|_\infty \right) \tag{3b}$$

$$\delta_\lambda \equiv \max\left(\left\| [(\lambda_{FA}^* + e)]^{-1} (\lambda_{FA} - \lambda_{FA}^*) \right\|_\infty \; \left\| [(\lambda_{FR}^* + e)]^{-1} (\lambda_{FR} - \lambda_{FR}^*) \right\|_\infty \right) \tag{3c}$$

$$\begin{aligned} \delta_\mu \equiv \max \Big(& \left\| \left[\left(\mu_{P\pm}^* + e \right) \right]^{-1} \left(\mu_{P\pm} - \mu_{P\pm}^* \right) \right\|_\infty \\ & \left\| \left[\left(\mu_{Q\pm}^* + e \right) \right]^{-1} \left(\mu_{Q\pm} - \mu_{Q\pm}^* \right) \right\|_\infty \\ & \left\| \left[\left(\mu_{V\pm}^* + e \right) \right]^{-1} \left(\mu_{V\pm} - \mu_{V\pm}^* \right) \right\|_\infty \\ & \left\| [(\mu_{SF}^* + e)]^{-1} (\mu_{SF} - \mu_{SF}^*) \right\|_\infty \\ & \left\| [(\mu_{ST}^* + e)]^{-1} (\mu_{ST} - \mu_{ST}^*) \right\|_\infty \Big). \end{aligned} \tag{3d}$$

In (3), e is the unitary vector and the $[\ldots]$ operator diagonalizes the enclosed vector. Small δ's indicate good solutions.

Traditionally, when optimizing the operation of a regulated power system, the objective function in (1) takes a simple smooth quadratic form. The electricity market, however, does not use quadratic cost because it does not cognitively match how market participants want to trade in the real world. Instead, non-differentiable piecewise cost based on offers and bids is adopted for better pricing transparency and flexibility. In this case, assuming only real energy cost is considered, the objective function can be written as

$$\begin{aligned} C(P) = & \sum_j \left\{ r_j^{m'} \left(P_j - d_j^{m'-1} \right) + \sum_m \left[r_j^m \left(d_j^m - d_j^{m-1} \right) \right] \right\} \\ & m \in \left\{ t | 1 \le t \le NB_j, d_j^t < P_j \right\} \end{aligned} \tag{4}$$

where r's represent offer prices, d's are the real power output levels at various breakpoints on the piecewise price curve ($d_0 \equiv 0$), NB is the number of real power blocks offered to the market from a given generator, and m' is by definition the block index that satisfies $d_j^{m'-1} < P_j < d_j^{m'}$. Fig. 1 illustrates an example

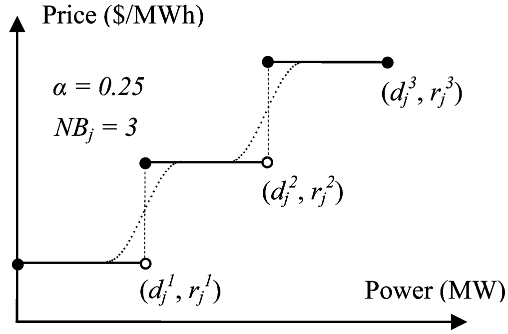

Fig. 2. Trigonometric smoothing of a discrete price-power curve.

price-power curve with four offer blocks. Costs for reactive energy, voltages, and other more complex resources and services can take similar forms.

These new piecewise cost functions presented in market-based OPFs bring computational difficulties. Existing NLP-based OPF algorithms such as PDIPM, in pursuing good performance, often take bold steps in updating trial solutions from iteration to iteration. When solving market-based OPF's in the form of (1) with non-differentiable piecewise objective functions like (4), these algorithms either break down or yield erroneous multipliers, because derivatives of the Lagrangian rise and fall abruptly around breakpoints of the underlying cost curves and destroy strong convergence properties. In the next two sections, we seek to address this issue with alternative algorithms and OPF formulations.

III. Alternative NLP-Based OPF Algorithms

For second-order NLP algorithms to work, we first need to smooth the objective function of the market-based OPF so that it can be differentiated. Let the price r be a piecewise linear function of the real power d as shown in (4) and Fig. 1, the smoothed price-power function r' and the corresponding objective function can be expressed as

$$C(P)=\sum_j \int_0^{P_j} r'_j(x)dx \tag{5a}$$

$$\begin{aligned} r'(d) &= r_+^m - r_-^m \cos\left[\pi\left(d-d_-^m\right)/\left(d_+^m-d_-^m\right)\right] \\ & \quad if\ d_-^m<d<d_+^m, \quad r(d), \text{otherwise} \\ r_\pm^m &\equiv \frac{1}{2}(r^{m+1}\pm r^m);\ d_\pm^m \equiv d^m-\alpha(d^m-d^{m\pm1}) \end{aligned} \tag{5b}$$

where $m \in [1, NB_j)$ and α is a positive number that controls the precision of the approximation. Fig. 2 shows a smoothed price-power curve along with its unmodified counterpart. Other piecewise costs can be smoothed in similar fashions.

A. Trust-Region Based Augmented Lagrangian Method

The augmented Lagrangian method (ALM) [21] solves a generic optimization problem

$$\begin{aligned} \min_X \quad & f(X) \\ \text{s.t.} \quad & H(X)=0; \quad G(X)\le 0 \end{aligned} \tag{6}$$

by converting it into a sequence of unconstrained optimization problems with penalty terms

$$\begin{aligned} \min_X L^k(X) &\equiv f(X)+(\lambda^k)^T H(X)+\frac{1}{2}H(X)^T[W^k]H(X) \\ &+\sum_{j=1}^{ni}\frac{1}{2U_j^k}\left\{\left(\max\left[\mu_j^k+U_j^kG_j(X),0\right]\right)^2-\left(\mu_j^k\right)^2\right\}. \end{aligned} \tag{7}$$

In (7), ni is the number of inequality constraints, λ^k and μ^k are trial Lagrange multipliers, and W^k and U^k are penalty parameters. In the so-called "multiplier method," λ^k, μ^k, W^k, and U^k are updated after each round of unconstrained optimization

$$\begin{aligned} \lambda^{k+1} &= \lambda^k+[W^k]H(X^k) \\ \mu_j^{k+1} &= \max\left\{\mu_j^k+U_j^kG_j(X^k),0\right\} \\ W_j^{k+1} &= \begin{Bmatrix} \beta_W W_j^k & if\ \left|H_j(X^k)\right|>\gamma_W\left|H_j(X^{k-1})\right| \\ W_j^k & if\ \left|H_j(X^k)\right|\le\gamma_W\left|H_j(X^{k-1})\right| \end{Bmatrix} \\ U_j^{k+1} &= \begin{Bmatrix} \beta_U U_j^k & if\ G_j(X^k)>\gamma_U G_j(X^{k-1}) \\ U_j^k & if\ G_j(X^k)\le\gamma_U G_j(X^{k-1}) \end{Bmatrix} \end{aligned} \tag{8}$$

where X^k is the solution of (7), $0<\gamma_W, \gamma_U<1$, and β_W, $\beta_U>1$. Convergence is achieved when

$$\begin{aligned} \left\|\nabla_X L_X(X^k)\right\| &\le \varepsilon^k \\ \|\lambda^{k+1}-\lambda^k\|/\left(1+\|\lambda^k\|_\infty\right) &\le \varepsilon_\lambda \\ \|\mu^{k+1}-\mu^k\|/\left(1+\|\mu^k\|_\infty\right) &\le \varepsilon_\mu \end{aligned} \tag{9}$$

are satisfied. In (9), the ε's are the tolerance parameters and ε^k decreases to a near-zero value ε^∞ as the suboptimization number k increases. Combined with a suitable unconstrained optimization algorithm, the augmented Lagrangian method can solve large-scale nonlinear constrained optimization problems very reliably and generate accurate Lagrangian multipliers.

In the TRALM algorithm, we use a trust-region method to solve (7). Trust-region methods represent a category of globally convergent unconstrained optimization algorithms [17]–[21]. Compared to the Newton's method, which was widely adopted in earlier OPF algorithms, trust-region methods are more robust in handling large-scale systems with indefinite starting points. Fundamentally, trust-region methods form and solve a sequence of simpler optimization problems within "trust regions" (the neighborhoods where the approximations remain valid) along the path that leads to the optimum. The pseudo code for the trust-region method adopted in TRALM is shown in Fig. 3, where Δ_0 is set according to [20] and X_0 is the X^k solved in the previous TRALM iteration. When solving the OPF with non-differentiable piecewise cost using TRALM, the difficulty resulting from abrupt changes of derivatives, as mentioned in Section II, is successfully mitigated by the automatic trust region sizing procedure. Large disruptive trial steps crossing breakpoints would result in small ρ's and hence get rejected and trigger the reduction of the trust-region size Δ.

Coleman *et al.* proposed a two-dimensional trust-region method for solving large-scale optimization problems [19], [20]. In their method, the trust region formed by $//S// \le \Delta$ in Fig. 3 is replaced with a two-dimensional region that spans the

Let $0 < \tau < \eta < 1$, $0 < \gamma_1 < 1 < \gamma_2$, $\Delta_0 > 0$,
  and X_0 be given, $t \leftarrow 0$
while $\| \nabla_X L(X_t) \| > \varepsilon$ **do**
  $\psi_t(S) \equiv \nabla_X L(X_t)^T S + \frac{1}{2} S^T \nabla_X^2 L(X_t) S$
  $S_t = \arg \min_{\|S\| \le \Delta_t} \psi_t(S)$
  $\rho_t = \dfrac{L(X_t + S_t) - L(X_t)}{\psi_t(S_t)}$
  if $\rho_t > \tau$, $X_{t+1} \leftarrow X_t + S_t$ **else** $X_{t+1} \leftarrow X_t$ **end if**
  if $\rho_t \le \tau$, $\Delta_{t+1} \leftarrow \gamma_1 \| S_t \|$
  else if $\rho_t > \eta$ **and** $\| S_t \| = \Delta_t$, $\Delta_{t+1} \leftarrow \gamma_2 \Delta_t$
  else $\Delta_{t+1} \leftarrow \Delta_t$ **end if**
  $t \leftarrow t + 1$
end do

Fig. 3. Pseudo code for the trust-region method adopted in TRALM.

gradient direction and the direction generated by the modified PCG or Cholesky procedure. Our experiments show, however, that neither the PCG nor the Cholesky variation of this 2-D trust-region method is capable of solving large-scale OPFs.

To solve the subproblem in Fig. 3, we use the algorithm documented in [18], which is essentially a Newton's procedure applied to solve for α in

$$\begin{aligned}\phi(\alpha) &\equiv \frac{1}{\Delta_t} - \frac{1}{\|S(\alpha)\|} = 0 \\ S(\alpha) &\equiv -\left(\nabla_X^2 L(X_t) + \alpha I\right)^{-1} \nabla_X L(X_t)\end{aligned} \tag{10}$$

where $\alpha \ge 0$ and $\nabla_X^2 L(X_t) + \alpha I$ is positive definite.

B. Step-Controlled Primal-Dual Interior Point Method

The primal-dual interior point method (PDIPM) and its many variations have become the algorithms of choice for solving OPFs over the past decade [7]–[13]. Given an optimization problem in the form of (6), PDIPM formulates the Lagrangian with barrier functions as

$$\begin{aligned}L^\gamma(X, Z, \lambda, \mu) \equiv f(X) &+ \lambda^T H(X) \\ &+ \mu^T (G(X) + Z) - \gamma \sum_{j=1}^{ni} \ln(Z_j)\end{aligned} \tag{11}$$

and uses the Newton's method to solve the KKT conditions

$$\begin{aligned}\nabla_X L^\gamma(X, Z, \lambda, \mu) = 0; &\quad H(X) = 0 \\ G(X) + Z = 0; &\quad [\mu] Z - \gamma e = 0\end{aligned} \tag{12}$$

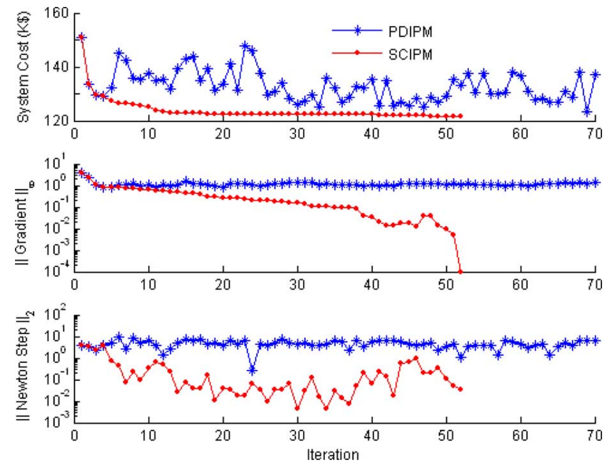

Fig. 4. Comparison of PDIPM and SCIPM in solving an 118-bus OPF with three-block piecewise linear cost.

where Z, μ, and γ are strictly positive. Each Newton step involves the solution of a reduced system of (12)

$$\begin{aligned}&\Delta Z = -G(X) - Z - \nabla G(X)^T \Delta X \\ &\Delta \mu = -\mu + [Z]^{-1} (\gamma e - [\mu] \Delta Z) \\ &\begin{bmatrix} M & \nabla H(X) \\ \nabla H(X)^T & 0 \end{bmatrix} \begin{bmatrix} \Delta X \\ \Delta \lambda \end{bmatrix} = \begin{bmatrix} -N \\ -H(X) \end{bmatrix} \\ &M \equiv \nabla_{XX}^2 L^\gamma(X, Z, \lambda, \mu) + \nabla G(X) [\mu] [Z]^{-1} \nabla G(X)^T \\ &N \equiv \nabla_X L^\gamma(X, Z, \lambda, \mu) + \nabla G(X) [Z]^{-1} ([\mu] G(X) + \gamma e).\end{aligned} \tag{13}$$

The variables (including γ) are updated according to

$$\begin{aligned}&\alpha_p = \min \left(\xi \min_{\Delta Z_j < 0} (-Z_j / \Delta Z_j), 1 \right) \\ &\alpha_d = \min \left(\xi \min_{\Delta \mu_j < 0} (-\mu_j / \Delta \mu_j), 1 \right) \\ &X \leftarrow X + \alpha_p \Delta X; Z \leftarrow Z + \alpha_p \Delta Z \\ &\lambda \leftarrow \lambda + \alpha_d \Delta \lambda; \mu \leftarrow \mu + \alpha_d \Delta \mu; \gamma \leftarrow \sigma (\mu^T Z)/ni\end{aligned} \tag{14}$$

where ξ and σ are constants that are typically set to 0.99995 and 0.1, respectively, in experiments.

Although PDIPM fits nicely with traditional OPFs that use smooth polynomial cost, we cannot count on it to solve market-based OPFs in the form of (1) with non-differentiable piecewise cost like (4), as demonstrated in the 118-bus OPF example shown in Fig. 4. When dealing with piecewise cost, the gradient and Hessian variables used in (12) and (13) change drastically from iteration to iteration. This causes a loss of the strong descending property of Newton steps.

The SCIPM algorithm shown in Fig. 5 overcomes this difficulty by monitoring the accuracy of the quadratic approximation of the Lagrangian during the OPF computation and shortening the Newton step if any sudden change of derivative results in an inaccurate approximation. Empirically, it is more efficient to start applying such step control procedure after the normal

Let $0 < \kappa < 1, 0 < \eta << 1, 0 < \varepsilon << 1,$

$X_0, Z_0, \lambda_0, \mu_0$, and γ_0 be given,

$L_t \equiv L^{\gamma_t}(X_t, Z_t, \lambda_t, \mu_t)$

$\psi_t(\Delta X_t) \equiv (\nabla_X L_t)^T \Delta X_t + \frac{1}{2}(\Delta X_t)^T (\nabla_X^2 L_t) \Delta X_t$

$\rho_t(\Delta X_t) \equiv \frac{L^{\gamma_t}(X_t + \Delta X_t, Z_t, \lambda_t, \mu_t) - L_t}{\psi_t(\Delta X_t)}$

$fcond_t \equiv \frac{\max(\max_{1 \le j \le ni}[G_j(X_t)], \| H(X_t) \|_\infty)}{1 + \max(\| \lambda_t \|_\infty, \| \mu_t \|_\infty)}$

$gcond_t \equiv \frac{\| \nabla_X L_t \|_\infty}{1 + \max(\| \lambda_t \|_\infty, \| \mu_t \|_\infty)}$

$ccond_t \equiv \frac{\mu_t^T Z_t}{1 + \| X_t \|_\infty}$

$ocond_t \equiv \frac{\| f(X_t) - f(X_{t-1}) \|}{1 + \| f(X_{t-1}) \|}$

$scipm \leftarrow false$

while $\forall cond \in (fcond_t, gcond_t, ccond_t, ocond_t) > \varepsilon$ **do**

compute $(\Delta X_t, \Delta Z_t, \Delta \lambda_t, \Delta \mu_t)$ according to (13)

if $scipm = true$

while $\rho_t(\Delta X_t) < 1 - \eta$ **or** $\rho_t(\Delta X_t) > 1 + \eta$ **do**

$\Delta X_t \leftarrow \kappa \Delta X_t; \Delta Z_t \leftarrow \kappa \Delta Z_t;$

$\Delta \lambda_t \leftarrow \kappa \Delta \lambda_t; \Delta \mu_t \leftarrow \kappa \Delta \mu_t;$

end do

end if

compute $(X_{t+1}, Z_{t+1}, \lambda_{t+1}, \mu_{t+1}, \gamma_{t+1})$ from

$(X_t, Z_t, \lambda_t, \mu_t, \gamma_t)$ and

$(\Delta X_t, \Delta Z_t, \Delta \lambda_t, \Delta \mu_t)$ according to (14)

if $fcond_{t+1} \ge fcond_t$ **and** $gcond_{t+1} \ge gcond_t$

$scipm \leftarrow true$

end if

$t \leftarrow t + 1$

end do

Fig. 5. Pseudo code for the step-controlled primal-dual interior point method.

PDIPM step fails to improve the gradient condition or the feasibility condition. Although Fig. 5 uses PDIPM as the baseline algorithm, the same step control concept applies to other interior point methods as well. As shown in Fig. 4, with step adjustments, SCIPM is able to reduce both system cost and gradients continuously.

TABLE I
EIGHT CATEGORIES OF CLASS-5 COMPOSITE NONSMOOTH OPTIMIZATION PROBLEMS CLASSIFIED ACCORDING TO THE THREE TESTS ON CONVEXITY, PIECEWISE LINEARITY, AND MINIMAX CONFORMITY

Category	Test 1	Test 2	Test 3
1	Yes	Yes	Yes
2 (Phantom)	Yes	Yes	No
3	Yes	No	Yes
4	Yes	No	No
5 (Phantom)	No	Yes	Yes
6	No	Yes	No
7	No	No	Yes
8	No	No	No

IV. ALTERNATIVE OPF FORMULATIONS

The problem in (1) with non-differentiable costs is essentially a Class-5 composite nonsmooth optimization problem [22]. We can divide this type of problems into the eight categories listed in Table I according to the following three tests:

1) whether the piecewise functions are strictly convex;
2) whether the piecewise functions are linear;
3) whether the problem is in a minimax form.

A Class-5 problem is a minimax problem if it is in the form of

$$\min_X f(X) \equiv \max_{i=1,\dots,n} f_i(X) \tag{15}$$

where each f_i is a smooth function. It is easy to see that, if a Class-5 problem passes Test 2, it would either pass both of the other two tests or fail both. Therefore, Categories 2 and 5 are phantom categories that do not need further considerations. Some problems in Table I do not present in today's market operations but may arise in the future when we embrace more flexible costings.

To solve the problems in Table I, one can take the algorithmic approaches introduced in Section III and apply global optimization techniques if necessary. Alternatively, for OPFs that fall into certain categories, the difficulty with non-differentiable piecewise cost may also be overcome by changing the problem formulation.

A. Decoupled Power Offers and Bids (DPOB) Formulation

In this formulation, which was adopted in [12] and [13], each block of generation offer or load bid presented on the original piecewise price curves is treated as the product of an independent generator or load unit and gets assigned a separate control variable. A given physical unit's contribution to the objective function therefore turns into the aggregate cost of several smoothly priced resources from smaller virtual units. Derivatives of the Lagrangian in turn become continuous in the higher-dimensional feasible region.

As indicted in [12], DPOB originates from separable programming [23]. This technique works well for problems from Categories 1, 3, and 4, whose piecewise functions are convex, like the ones shown in Fig. 1.

B. Constrained Cost Variables (CCV) Formulation

For problems from Categories 1, 3, and 7, which are in minimax forms, constrained cost variables can be introduced to turn

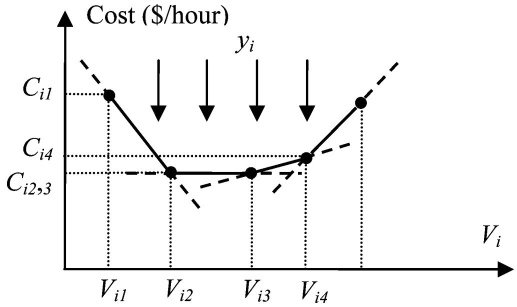

Fig. 6. Modeling voltage cost curve using constrained cost variables.

the nonsmooth optimization problems into smooth ones [24]. To the best of our knowledge, this method has not been applied to the solution of OPFs in the past. In CCV, each piecewise function in the objective is replaced with a helper variable. Several accompanying inequality constraints, one for each piece of the piecewise function, are then placed on that variable. The new constraints build a convex basin equivalent to requiring the helper cost variable to lie in the epigraph of the cost curve. A simple term summating all helper cost variables replaces piecewise cost terms in the original objective function. When the new objective function is minimized, helper cost variables will be pushed against basins. Fig. 6 illustrates the CCV concept for a piecewise voltage cost curve. In this example, y_i is the helper cost variable that replaces the piecewise cost term related to the voltage V_i in the objective function. The four accompanying constraints are

$$m_{iv}(V_i - V_{iv}) + C_{iv} - y_i \leq 0 \quad \text{for } v = 1, \ldots, 4 \tag{16}$$

where m_{iv}'s are slopes of the four cost curve segments. The new objective function is written as

$$C(P, Q, V, \theta, y) = C(P, Q, V, \theta) + \sum_i y_i \tag{17}$$

where C' abstracts other cost terms.

Like DPOB, CCV overcomes the difficulty of disruptive Lagrange derivatives by extending the optimization into a higher dimensional space and counting on good constrained optimization techniques such as PDIPM to solve the transformed smooth optimization problem.

V. Numerical Results

We tested the new OPF formulations and algorithms using several power system models that are summarized in Table II. Tests were run on a PC with Intel 3.3 GHz P4 processor (2 MB L2 cache), 2 GB memory, and Linux 2.6.9 kernel. All optimization programs and underlying linear algebra functions, except the LU and Cholesky factorization modules, were developed in house using Standard C and compiled using the GCC 3.4.4 compiler. LU and Cholesky factorizations were done using the UFsparse package [25]. The parameters used in PDIPM, TRALM, SCIPM, and cost-curve smoothing, unless stated otherwise, were set according to Table III. All experiments use flat starting points, i.e., unit voltages, zero phase angles, and generator outputs at the midpoints between maximum generations and minimum generations. Offers and bids for energy and voltages were randomly generated.

TABLE II
Summary of Power System Models Used in the Study

System	Buses	Generators	Branches	Load (MW)
1	30	6	41	189
2	57	7	80	1,250
3	118	54	186	4,242
4	300	69	411	23,525
5	2383	327	2896	24,558
6	2935	956	7028	394,794

TABLE III
Parameters Used in PDIPM, TRALM, SCIPM, and Trigonometric Smoothing of Piecewise Linear Cost Curves

$NB = 3,\ \alpha = 0.04$							
TRALM				PDIPM/SCIPM			
ε_λ	5e-3	τ	0.25	κ	0.5	Z_0	1.0
ε_μ	1e-1	η	0.75	η	0.1	λ_0	0.0
ε^0	2e0	γ_1	0.1	ε	1e-5	μ_0	1.0
ε^∞	1e-2	γ_2	2.0	X_0	flat start	γ_0	1.0
$\beta_{W,U} = 3$		$\gamma_{W,U} = 0.33$		$\xi = 0.99995$		σ	0.1

TABLE IV
Comparison of Execution Time (seconds) and Numbers of Iterations (Shown in Parenthesis) of Four Algorithms in Solving OPFs

Solving OPF's with Quadratic Costs				
System	MINOS	PDIPM	TRALM	SCIPM
1	0.06 (350)	0.05 (13)	0.20 (134)	0.07 (13)
2	0.07 (179)	0.11 (14)	0.40 (146)	0.17 (17)
3	1.2 (1579)	0.37 (21)	2.3 (441)	0.57 (24)
4	6.3 (3654)	1.2 (29)	4.8 (420)	1.3 (24)
5	FAIL	12 (33)	168 (1834)	14 (33)
6	FAIL	22 (34)	680 (2842)	26 (34)
Solving OPF's with Piecewise Costs				
System	MINOS	PDIPM	TRALM	SCIPM
1	0.04 (163)	0.66 (171)	0.34 (221)	0.15 (26)
2	0.07 (184)	0.93 (126)	0.40 (171)	0.47 (45)
3	0.9 (1190)	FAIL	3.7 (698)	1.9 (77)
4	3.8 (2002)	27 (689)	6.7 (544)	4.0 (72)
5	FAIL	FAIL	202 (2193)	54 (122)
6	FAIL	FAIL	1011 (4310)	161 (204)

At the time of writing, we are not able to find an appropriate production-quality OPF tool with which to compare our new formulations and algorithms. (The lack of a robust commercial AC OPF tool has been a major hurdle for the market to institute advanced options of trading ancillary services such as reactive power [16].) Instead, comparisons are made among the different formulations and algorithms presented in this paper and against the MINOS used in MATPOWER [26], [27] and our own implementation of PDIPM.

A. Convergence and Performance

Table IV lists the performance comparison of four algorithms in computing classically formulated OPFs. TRALM and SCIPM converged in all cases, while MINOS failed to solve large-scale

TABLE V
COMPARISON OF EXECUTION TIME (seconds) AND NUMBERS OF ITERATIONS (SHOWN IN PARENTHESIS) OF SOLVING DIFFERENTLY FORMULATED OPFs

OPF's with Convex Piecewise Linear Costs			
System	Classical-SCIPM	DPOB-PDIPM	CCV-PDIPM
1	0.15 (26)	0.06 (13)	0.06 (15)
2	0.47 (45)	0.11 (13)	0.17 (22)
3	1.9 (77)	0.39 (19)	1.9 (109)
4	4.0 (72)	1.3 (30)	1.2 (28)
5	54 (122)	13 (35)	15 (43)
6	161 (204)	32 (47)	49 (78)

TABLE VI
ACCURACIES OF OPF SOLUTIONS COMPUTED BY DIFFERENT ALGORITHMS (300-BUS SYSTEM, MINOS AS THE REFERENCE)

Algorithm	δ_C	δ_X	δ_λ	δ_μ
TRALM	5.2e-4	2.6e-2	1.6e-3	9.0e-3
SCIPM	5.2e-4	2.7e-2	1.6e-3	8.6e-3
DPOB-PDIPM	2.9e-7	1.3e-3	1.0e-4	3.6e-4
CCV-PDIPM	7.1e-5	5.4e-4	5.5e-5	8.6e-5

OPFs and PDIPM failed to solve market-based OPFs with piecewise costs. SCIPM is faster than TRALM and better suited for real-time applications.

One theoretical pitfall of SCIPM, like that of PDIPM, is its lack of global convergence guarantee. In [12], the authors showed some of PDIPM's failures and proposed an algorithm that attempted to improve the convergence at the cost of performance through adjustments of Hessian matrices. Our investigation showed, however, that it is the OPF formulation in [12], which treats all constraints as inequality constraints, that brings numerical difficulties to PDIPM in the case of solving large-scale OPFs. Using the formulation in (1), we were not able to regenerate any non-converging results reported in [12]. SCIPM, as well as PDIPM in the context of OPFs with quadratic costs, consistently converges to desired OPF solutions, with both the first-order and the second-order KKT conditions satisfied. These encouraging results may imply that the region of attraction for our particular nonlinear system is large enough to counter occasional ill-defined Newton steps.

Table V compares three different OPF formulations in the solution of market-based OPFs, with PDIPM or SCIPM as the underlying algorithm. DPOP and CCV clearly provide better performances, although the Classical-SCIPM approach has the advantage of being extendable to solve problems in Category 8.

B. Accuracy

Table VI lists the result of a cross examination of OPF solutions generated by MINOS, TRALM, SCIPM, DPOB-PDIPM, and CCV-PDIPM. As defined in Section II, δ_C, δ_X, δ_λ, and δ_μ measure the deviation of a trial OPF solution from the reference one. The small values reported in Table VI indicate that all methods proposed are valid for computing large-scale market-based OPFs.

The parameter α used in (5) has an impact on the accuracies of TRALM and SCIPM's solutions. As shown in Table VII, smaller α's yield more accurate solutions. In practice, 0.04 is small enough to ensure satisfactory results.

TABLE VII
ACCURACIES OF SEVERAL OPF SOLUTIONS COMPUTED BY SCIPM WITH DIFFERENT α VALUES (300-BUS SYSTEM, CCV-PDIPM AS THE REFERENCE)

α	δ_C	δ_X	δ_λ	δ_μ
0.1	1.3e-3	4.6e-2	3.6e-3	2.4e-2
0.04	5.2e-4	2.7e-2	1.6e-3	8.6e-3
0.01	1.3e-4	6.9e-3	4.1e-4	2.1e-3

TABLE VIII
EXECUTION TIME (seconds) AND NUMBERS OF ITERATIONS TAKEN TO SOLVE THE 2935-BUS OPF WITH DIFFERENT NB VALUES

SCIPM					
NB	# Its.	Time	*NB*	# Its.	Time
3	204	161	4	218	173
5	217	172	6	263	210
7	323	263	8	344	278
9	362	292	10	402	328
DPOB-PDIPM					
NB	# Its.	Time	*NB*	# Its.	Time
3	47	32	4	48	33
5	46	33	6	48	35
7	47	35	8	45	35
9	46	36	10	46	37
CCV-PDIPM					
NB	# Its.	Time	*NB*	# Its.	Time
3	78	49	4	98	61
5	72	46	6	98	62
7	76	49	8	87	56
9	74	48	10	97	62

C. Scalability

The time taken to solve an OPF depends on both the number of iterations taken and the computational complexity of one single iteration. Assuming a constant transmission network density and a constant fill-in ratio for the sparse matrix factorization, the complexities of one iteration of PDIPM, TRALM, and SCIPM are all $O(N_{\text{bus}})$, although their underlying coefficients are quite different. Although the exact relationship between the system size and the number of iterations is unclear, we can identify some general trends from Tables IV and V. First of all, the number of iterations generally rises as the system size increases. Second, the rising paces for PDIPM and SCIPM are much slower than those of MINOS and TRALM, suggesting that SCIPM and CCV-PDIPM are more scalable and therefore better suited for large-scale systems. Third, other system details (such as number of generators) also have an impact on the algorithm complexity. Omitting those system-specific characteristics, the overall OPF complexity can be approximated by $O(N_{\text{bus}}^{1+\varepsilon})$, where ε is a small number that falls between 0.1 and 0.2 for SCIPM and CCV-PDIPM.

The number of segments contained in piecewise cost curves also impacts the performance of second-order NLP-based OPF algorithms. Table VIII lists the execution time and numbers of iterations taken by SCIPM, DPOB-PDIPM, and CCV-PDIPM to solve the 2935-bus OPF with different NB values. The number of iterations taken by SCIPM grows approximately linearly with

NB, while those by DPOB-PDIPM and CCV-PDIPM are insensitive to NB. We should note that DPOB and CCV's scalabilities are limited to relatively small NB's. For large NB's, DPOB dictates dense $\nabla H(X)$'s and is therefore unscalable both in terms of speed and in terms of memory requirement. CCV, on the other hand, does not encounter such a problem, because each accompanying constraint that it adds to the problem only contains a small and fixed number of variables. Depending on the underlying computing platform used, the extra memory required by CCV to accommodate new inequality constraints and helper cost variables may or may not be an issue. All that said, we do not need to worry about DPOB and CCV's scalabilities for today's electricity market operations, where NB's are often capped around 10∼20. In the future, however, computerized fine-grain trading could be instituted and present a challenge to the two alternative formulations.

VI. Conclusions

In this paper, we discussed the computational challenges posed by the electricity market and proposed three new techniques (TRALM, SCIPM, and CCV) to address them. Numerical studies showed that these techniques are reliable and better than some existing ones in solving large-scale market-based nonsmooth OPFs. DPOB-PDIPM and CCV-PDIPM are particularly good for real-time applications due to their efficiencies, while SCIPM and TRALM can be applied to solve problems that cannot be reformulated through DPOP or CCV. When dealing with non-convex cost, however, the methods discussed in this paper must be combined with global optimization techniques, in order to achieve global optimal solutions. In the future, we need to pay attention to DPOB and CCV's large memory requirements as the market embraces finer-grain electricity trading. Future research should put more emphasis on OPF robustness, accuracy, and scalability, in light of the changing roles of OPF in market-oriented applications. We plan to discuss how to integrate the new formulations and algorithms into the security-constrained OPF in the future.

References

[1] J. Carpentier, "Contribution a l'Etude du Dispatching Economique," *Bull. Soc. Francaise des Electriciens*, vol. 3, pp. 431–447, Aug. 1962.

[2] O. Alsac and B. Stott, "Optimal load flow with steady-state security," *IEEE Trans. Power App. Syst.*, vol. PAS-93, no. 3, pp. 745–751, May/Jun. 1974.

[3] B. Stott, O. Alsac, and A. J. Monticelli, "Security analysis and optimization," *Proc. IEEE, Special Issue on Computers in Power System Operations*, vol. 75, no. 12, pp. 1623–1644, Dec. 1987.

[4] O. Alsac, J. Bright, M. Prais, and B. Stott, "Further developments in LP-based optimal power flow," *IEEE Trans. Power Syst.*, vol. 5, no. 3, pp. 697–711, Aug. 1990.

[5] J. Carpentier and P. Bornard, "Towards an integrated secure optimal operation of power systems," in *Proc. 1991 IEE Int. Conf. Advances in Power System Control, Operation, Management*, vol. 1, pp. 1–16.

[6] M. Huneault and F. D. Galiana, "A survey of the optimal power flow literature," *IEEE Trans. Power Syst.*, vol. 6, no. 2, pp. 762–770, May 1991.

[7] S. Granville, "Optimal reactive dispatch through interior point method," *IEEE Trans. Power Syst.*, vol. 9, no. 1, pp. 136–146, Feb. 1994.

[8] Y. Wu, A. S. Debs, and R. E. Marsten, "A direct nonlinear predictor-corrector primal-dual interior point algorithm for optimal power flows," *IEEE Trans. Power Syst.*, vol. 9, no. 2, pp. 876–882, May 1994.

[9] G. L. Torres and V. H. Quintana, "Optimal power flow by a nonlinear complementarity method," *IEEE Trans. Power Syst.*, vol. 15, no. 3, pp. 1028–1033, Aug. 2000.

[10] G. L. Torres and V. H. Quintana, "On a nonlinear multiple-centrality-corrections interior-point method for optimal power flow," *IEEE Trans. Power Syst.*, vol. 16, no. 2, pp. 222–228, May 2000.

[11] E. D. Castronuovo, J. M. Campagnolo, and R. Salgado, "On the application of high performance computation techniques to nonlinear interior point methods," *IEEE Trans. Power Syst.*, vol. 16, no. 3, pp. 325–331, Aug. 2001.

[12] R. A. Jabr, A. H. Coonick, and B. J. Cory, "A primal-dual interior point method for optimal power flow dispatching," *IEEE Trans. Power Syst.*, vol. 17, no. 3, pp. 654–662, Aug. 2001.

[13] W. Qiu, A. J. Flueck, and F. Tu, "A new parallel algorithm for security constrained optimal power flow with a nonlinear interior point method," in *Proc. 2005 IEEE Power Eng. Soc. General Meeting*, pp. 2422–2428.

[14] *"PJM Manual 06, 11, 12: Scheduling Operations."* [Online]. Available: http://www.pjm.com/contributions/pjm-manuals/manuals.html.

[15] C. E. Murillo-Sanchez, "On the integration of unit commitment and optimal power flow," Ph.D. dissertation, School Elect. Comput. Eng., Cornell Univ., Ithaca, NY, 2000.

[16] Federal Energy Regulatory Commission, "Principles for efficient and reliable reactive power supply and consumption," FERC Staff Reports, Docket No. AD05-1-000, pp. 161–162, Feb. 2005. [Online]. Available: http://www.ferc.gov/legal/staff-reports.asp.

[17] D. Gay, "Computing optimal locally constrained steps," *SIAM J. Sci. Stat. Comput.*, vol. 2, pp. 186–197, Jun. 1981.

[18] J. J. More and D. C. Sorensen, "Computing a trust region step," *SIAM J. Sci. Stat. Comput.*, vol. 4, pp. 553–572, Sep. 1983.

[19] T. F. Coleman and Y. Li, "An interior trust region approach for nonlinear minimization subject to bounds," *SIAM J. Optim.*, vol. 6, pp. 418–445, May 1996.

[20] M. A. Branch, T. F. Coleman, and Y. Li, "A subspace, interior, and conjugate gradient method for large-scale bound-constrained minimization problems," *SIAM J. Sci. Comput.*, vol. 21, pp. 1–23, Aug. 1999.

[21] D. P. Bertsekas, *Nonlinear Programming*, 2nd ed. Nashua, NH: Athena Scientific, 1999, pp. 95–97, 397-426.

[22] R. S. Womersley and R. Fletcher, *J. Optim. Theory Appl.*, vol. 48, pp. 493–523, Mar. 1986.

[23] M. S. Bazaraa and C. M. Shetty, *Nonlinear Programming—Theory and Algorithms*. New York: Wiley, 1979, pp. 453–471.

[24] R. Fletcher, *Practical Methods of Optimization*, 2nd ed. New York: Wiley, 1987, pp. 357–416.

[25] [Online]. Available: http://www.cise.ufl.edu/research/sparse/UFsparse.

[26] R. D. Zimmerman, C. E. Murillo-Sanchez, and D. Gan, MATPOWER 3.0.0 User's Manual. [Online]. Available: http://www.pserc.cornell.edu/matpower.

[27] B. D. Murtagh and M. A. Saunders, MINOS 5.5 User's Guide, Stanford University Systems Optimization Laboratory, Tech. Rep. SOL83-20R.

Hongye Wang (S'99) received the B.S. degree in physics from Jilin University, Changchun, China, in 1998, and the M.S. degree in electrical engineering from Cornell University, Ithaca, NY, in 2001. He is currently pursuing the Ph.D. degree in the School of Electrical and Computer Engineering at Cornell University.

From 2001 to 2004, he worked at Nortel Networks and UTStarcom Inc. as a Software Engineer and a System Engineering Manager. He conducts research on computational issues associated with the design and operations of electricity markets.

Carlos E. Murillo-Sánchez (M'87) studied electronics engineering at Instituto Tecnológico y de Estudios Superiores de Monterrey, Mexico. He then studied at the University of Wisconsin-Madison, where he received the M.S. degree in electrical engineering and control systems. He received the Ph.D. degree in from Cornell University, Ithaca, NY, in December 1999.

He worked in several universities in Mexico and Colombia before enrolling at Cornell, where he has been a Postdoctoral Associate and a Visiting Scientist in the School of Electrical and Computer Engineering at Cornell University. Currently, he is a tenured Professor and Dean of Engineering at Universidad Autónoma de Manizales, Manizales, Colombia. His interests include power systems operation, control and markets, control systems applications, optimization, and simulation.

Dr. Murillo-Sánchez is a founding member of the Asociación Colombiana de Automática.

Ray D. Zimmerman (M'91) is a Senior Research Associate in electrical engineering and applied economics at Cornell University. He is Director of the Laboratory for Experimental Economics and Decision Research. His current research interests center on the interactions between the economic and engineering aspects of electric power industry restructuring. Other interests include software tools for education and research. He is the primary developer of the two simulation tools MATPOWER and POWERWEB.

Robert J. Thomas (M'73–SM'83–F'93) currently holds the position of Professor of electrical and computer engineering at Cornell University, Ithaca, NY. His technical background is broadly in the areas of systems analysis and control of large-scale electric power systems. He has published in the areas of transient control and voltage collapse problems as well as technical, economic, and institutional impacts of restructuring.

Dr. Thomas has been a member of the IEEE-USA Energy Policy Committee since 1991 and was the committee's Chair from 1997 to 1998. He has served as the IEEE-USA Vice President for Technology Policy. He was a member of the USDOE Secretary's Power Outage Study Team in 2003 and the August 14, 2003 Blackout Investigation Team. He is a member of Tau Beta Pi, Eta Kappa Nu, and Sigma Xi.